International Journal of Nanoelectronics and Materials
Volume 13 (Special Issue) May 2020 [379-392]

Experimental and Numerical Investigation on the Role of Double Helical Angle Tool in Trimming CFRP Aerospace Composites

R. Izamshah[1*], S. A. Suandi[1], M. Akmal[1], M. F. Jaafar[1], M. S. Kasim[1], S. Ding[2] and M. H Hassan[3]

[1]*Advanced Manufacturing Centre, Universiti Teknikal Malaysia Melaka, Hang Tuah Jaya, 76100 Durian Tunggal, Melaka, Malaysia.*
[2]*School of Engineering, RMIT University, VIC 3083, Australia.*
[3]*Gandtrack Asia Sdn. Bhd., Jalan TU 2, MITC Industrial Park, 75450 Ayer Keroh, Melaka, Malaysia.*

ABSTRACT

Carbon fiber reinforced polymers (CFRP) is extensively used in aircraft structure due to its superior physical and mechanical properties. Since it is necessary to perform the edge-trimming operation for removal of the remaining materials after the curing to net shape, it is critical to study the role of tool geometry with contemplation to improve the edge-trimmed quality. The present research aims to investigate the effects of left and right helical angle in edge-trimming CFRP composite with the help of computational statistical modelling and numerical simulation. Based on the response surface methodology (RSM) and analysis of variance (ANOVA) results, it was found that both left and right helix are statistically significant on surface roughness and unintentionally blended to form segmented helical edge. Furthermore, the observation on the simulation results revealed that CFRP plies experienced two directions of forces which were downward forces by effects of right helix and upward forces by effects of left helix. Additionally, the left helix serves as a secondary material remover which removed the residue material left by right helix. This study provides an information that can offer great prospective for new optimum tool design.

Keywords: Precision Machining, Double Helical Tool, CFRP, Finite Element Analysis.

1. INTRODUCTION

The use of carbon fibre reinforced plastic (CFRP) in aerospace, naval and automotive industries application have ultimately increased over the last decade. This near net-shape engineered composite material offers an excellent strength and modulus together with low density, low coefficient of thermal expansion, excellent in fatigue and high corrosion resistance [1]. In general, it is compulsory to perform a post-machining operation such as edge-trimming after de-moulding of the CFRP parts in order fulfil the tolerances requirement for fitting and joining the parts purposed [2].

However, edge-trimming of CFRP material is known to be a challenging process due to the cutting properties of this material that are influenced by the heterogeneity and anisotropy structures [3]. Some of the defects of edge-trimming operations are delamination [4], burr formation [5] and poor surface quality [6]. In order to reduce the probability of these defects and acquire the tolerable parts quality, many of the researchers have given an insight regarding machinability of CFRP [2, 3]. However, they often neglect the effects of tool geometrical features which are vital to the machining performances.

*Corresponding Author: *izamshah@utem.edu.my*

With the advancement of computational technology either for statistical analysis or numerical analysis, they have a profound effect for scientific research. The practice for statistical analysis by employing response surface methodology (RSM) being associated with computer assisted data analysis, is capable of reducing the number of experiments with benefits of a wide coverage with optimal factor region [8,9, 10].

The complexity in today's engineering applications has motivated several works employing numerical analysis [11, 12, 13]. Numerical simulation offers a solution for any complex performance issues that are difficult to be achieved by experimental works due to its high cost and time. The drawbacks of fast tool wear and poor surface finish in composite machining due to the continuous contact of the tool and workpiece makes the numerical simulation become an alternative approach to develop an understanding on the behaviour of composite machining [14]. Modelling and simulation of edge-trimming operations have the potential for improving tool designs especially in composite machining. In this study, an attempt has been made to investigate the role of double helical angle for cross-nick tool in trimming CFRP composites. This research contains two sections of results which are, an experimental investigation on the effects of double helix angle on surface roughness followed by the visualisation results of numerical simulation in illustrating the roles of the left and right angle toward the plies behaviour.

2. MATERIALS AND METHODS

2.1 Experimental Design

The research methodology can be divided in two categories namely statistical analysis and finite element analysis. A central composite design (CCD) has been employed in the present study to establish comprehensive experimental investigation. The design matrix has been generated and analyzed by using software Design-Expert. The selected rotatable of the CCD design with alpha (α) value =1.414 contains 2^k of factorial points, 2k of axial points (alpha value-α) and three center-points to represent the replication, k represents the number of variables. Therefore, the total of eleven cutting tools were developed in this research study. Table 1 presents the design matrix and the results of surface roughness for this research study.

Table 1 Experimental design matrix of rotatable CCD with surface roughness results

Standard Order	Trials Number	Helix Left (degree°)	Helix Right (degree°)	Surface Roughness (μm)
11	1	10	40	3.58
2	2	12	35	1.29
6	3	13	40	5.44
3	4	8	45	1.85
7	5	10	33	2.78
9	6	10	40	3.60
5	7	7	40	3.70
1	8	8	35	2.40
4	9	12	45	6.51
10	10	10	40	3.34
8	11	10	47	1.47

The second order of polynomial model has been used to describe the relationship between the independent variable and the response variable as follows:

$$Y = \beta_0 + \sum_{i=1}^{n} \beta_i X_{iu} + \sum_{i=1}^{n} \beta_{ii} X^2{}_{iu} + \sum_{i<j} \beta_{ij} X_{iu} X_{ju} + e_u \quad (1)$$

where *Y* is the desired response, β_0 is ~~a~~ the constant, β_i, β_{ii} and β_{ij} represent the coefficients of linear, quadratic, and interaction variables. X_i indicates the coded value of the corresponding study variables.

The statistical significance of each variable and the fitness of response model was evaluated by the analysis of variance (ANOVA). The results of the ANOVA are presented in Table 2. According to Table 2, the response model proposed match the results of surface roughness in terms of satisfactory results of the coefficient of determination (R^2), adequate precision and the model possesses no significant lack of fit. The lack of fit test are used to identify the significant variable left out in the response model, the not significant lack of fit implies that the variables have considerable influence on the response and none of the significant variable is left out of the model [15]. R^2 represents how close the data is to the fitted regression line. Predicted R^2 represents the ability of the model to predict the new set of data. Thus, the response model is built as follows.

$$\text{Surface Roughness (μm)} = -304.59 + 57.89(\text{Helix Left}) + 9.11(\text{Helix Right}) - 1.49(\text{Helix Left} \times \text{Helix Right}) - 3.17\ (\text{Helix Left})^2 - 3.087\times 10^{-4}(\text{Helix Right})^2 + 8.177 \times 10^{-4}((\text{Helix Left})^2 \times (\text{Helix Right})^2) \quad (2)$$

Based on the ANOVA results in (Table 2), all individual variables and its interaction possess statistically significant surface roughness results with p-value < 0.05. These results indicate that both, helical features in the cross-nick tool either the left or right helix, influences the results of surface roughness.

Table 2 ANOVA for response model

Source	Sum of Squares	Degree of freedom	Mean Square	F Value	p-value Prob > F	
Model	25.39	6	4.232	43.961	0.0013	significant
A-Helix Left	4.464	1	4.464	46.376	0.0024	
B-Helix Right	0.858	1	0.858	8.914	0.0405	
AB	8.323	1	8.323	86.466	0.0007	
A^2	1.214	1	1.214	12.611	0.0238	
B^2	3.208	1	3.208	33.328	0.0045	
A^2B	5.295	1	5.295	55.005	0.0018	
Residual	0.385	4	0.096			
Lack of Fit	0.343	2	0.172	8.197	0.1087	not significant
Pure Error	0.042	2	0.021			
Cor Total	25.775	10				
Standard Deviation	0.31		R^2	0.985		
Mean	3.269		Adjusted R^2	0.963		
C.V. %	9.491		Predicted R^2	0.771		

PRESS	5.899	Adequate Precision	21.091

2.2 Experimental setup

In this present study, a total of eleven cross-nick tools with different helical geometrical features were fabricated in-house using CNC Michael Deckel tool and cutter grinder machine as referred to in the CCD design matrix (Table 1). The detailed specifications and fixed geometrical feature i.e. dimension, rake angle, clearance angle and the number of flutes for the cross-nick tool are presented in Table 3. Table 4 shows an example of the cross-nick tool that was fabricated and used in this present study.

Table 3 Cross nick tool specification and fixed geometrical parameter

Tool Material	Micro grain K20 Tungsten Carbide
Dimension	Diameter=8 mm, Length=70 mm
Rake Angle	10°
Clearance Angle	65°
Flutes	8

Table 4 Cross-nick tool with different helical feature fabricated

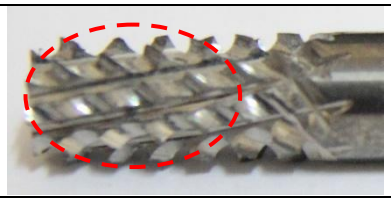	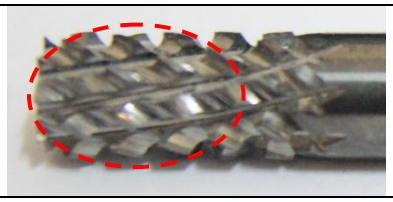
(a) Left-10˚, Right-40˚	(b) Left-12˚, Right-35˚
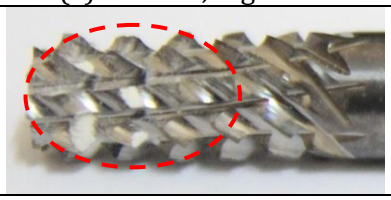	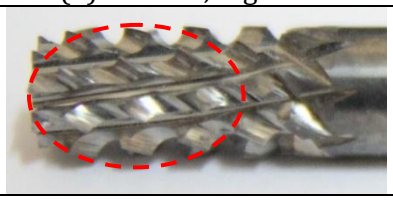
(c) Left-13˚, Right-40˚	(d) Left-7˚, Right-40˚

The experiment was carried out under the dry cutting conditions on HAAS CNC milling machine with up-mill configuration with the benefits of low engagement force and the prevention of workpiece lifted compared to the down-mill. Figure 1 shows the actual experimental setup and the numerical model for tool and workpiece in this research works. The cutting speed used for the edge-trimming process was 176 m/min and with a feed of 0.2 mm/tooth. The width of cut is 4 mm and 100 mm of the machining length. The CFRP was workpiece clamped by using a strap clamp and equipped with a dust vacuum for removing the CFRP debris. The overhang of the workpiece is about 15 mm.

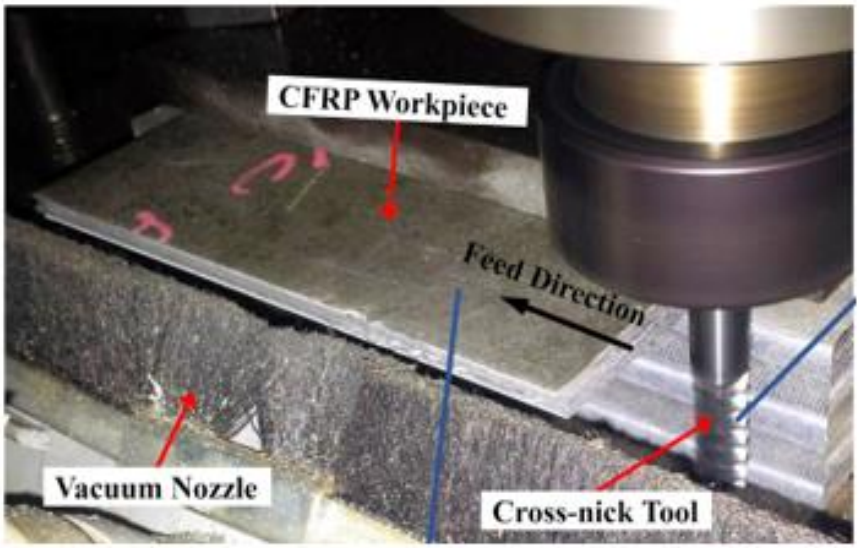

(a)

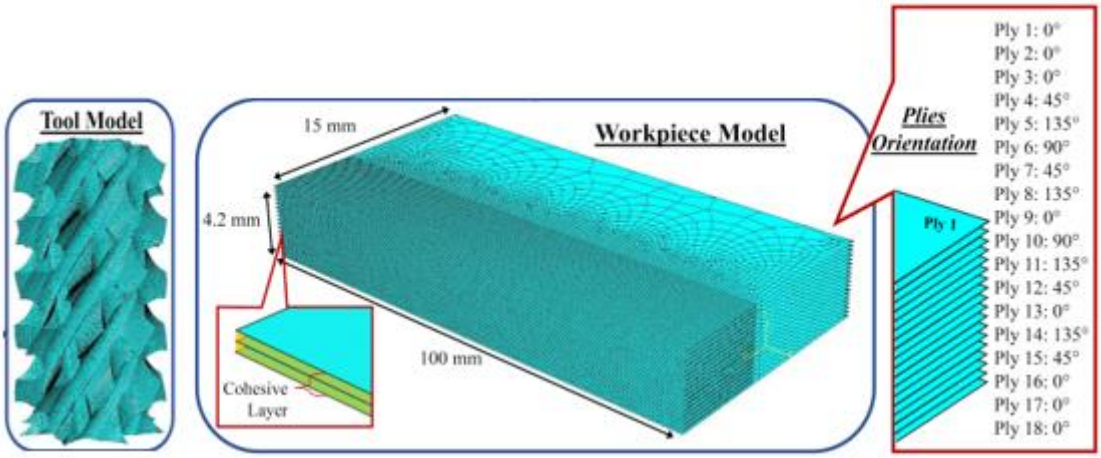

(b)

Figure 1. (a) Edge-trimming experimental setup, (b) modelling of tool and CFRP part.

2.3 Finite Element Modelling for Edge-Trimming Process

The cross-nick tool was modelled by using shell element with 56 411 rigid mesh elements (R3D3, 4 node 3-D bilinear rigid quadrilateral). Shell element offers huge computational time savings compared to solid element. The CFRP is meshed by using a multi-layer four-node linear shell element with reduced integration, automatic hourglass control and finite membrane strains (element type S4R), 170 946 number of mesh elements and an interface delamination model was generated to simulate the composite behaviour by allowing the cohesive bonding surface between each ply. The other information about CFRP as materials has been provided in Table 5.

The mesh density on the edge-trimming zone has been designed to be fine for enhancing the accuracy of the results but the mesh was kept coarse out of this zone in order to reduce the computational time. An element deletion method also has been employed to allow the element separation among the nodes to form the chip. As soon as the elastic stiffness of the examined nodes element is degraded to zero, the elements would be deleted automatically from the other nodes element which allows the separation of CFRP material in forming the chips [16]. The plies

orientation of the CFRP workpiece has been assigned using *Material Orientation* software feature.

Table 5 Workpiece material specification

Materials	Carbon Fibre Reinforced Polymer (CFRP)
Type	Laminate
Number of Plies	18
Size	Length= 100 mm, Width= 100 mm and Thickness= 4.6 mm
Orientation	0°, 45°,90°,135° (Details referred Figure 1)

In the present study, the numerical simulation is used to identify the influences of the left and right helix on the plies and fibres of CFRP composite during engagement by the cross-nick tool. The simulation results covered the observations of damage progression made by helical features of the cross-nick tool. In summary, the following assumptions were made:

i. The cross-nick tool is assumed rigid
ii. During the edge-trimming process, the workpiece was able to deform and deflect to any degree of freedom
iii. The results only focused on plies and the fibre behavior, therefore the properties and results of temperature and force were neglected

In order to model the characteristic of the CFRP material for numerical simulation, the laminate model with surface-to-surface-contact of cohesive layer and damage properties has been used specific to *Cohesive Behaviour* in *Contact Property Options* at ABAQUS software. The cohesive behaviour of surface to surface contact are identified through cohesive stiffness in three directions (*Knn=Kss=Ktt* = 10^5 N/mm^2) [17].

For carbon woven fibre material properties, the Johnson-cook fracture model has been used to represent carbon woven plies after many experiments. By comparing with Hashin's damage model [18, 19] which is known to be a suitable damage model for composite in finite element modelling, the workpiece model is essentially assigned as a solid material because of its behaviour towards damage materials that possess characteristics of fibre tensile and compressive failure and matrix crack [20]. Therefore, this damage model is not suitable to be used with its cohesive behaviour in this present study. The results of employing this method led to the plies and fibres deformation unable to be seen clearly during the engagement of cross-nick tool to the CFRP workpiece. Besides, the cohesive bonding failed earlier before the fibres which does not happens in the real experimental works.

Therefore, the coefficient used for the heterogeneous approach is based on the assumption that the carbon woven is a very brittle material. In order to obtain a realistic illustration of the deformation and fracture response for the Johnson-cook fracture damage model, the coefficient of d1 and d2 are set very low. Table 6 provides information about general properties of CFRP and Johnson-cook damage model, which is used for modelling the CFRP material. The Johnson-cook model covered plasticity and damage initiation element. The plasticity model prescribes the dependency of plastic flow stress $(\underline{\sigma})$ on equivalent plastic strain (ε_p), equivalent plastic strain rate ($\dot{\varepsilon}$), and the homologous temperature (T^*):

$$\underline{\sigma} = \left(A + B\varepsilon_p^n\right)\left(1 + C\ ln\ ln\ \frac{\dot{\varepsilon}}{\dot{\varepsilon}_0}\right)[1 - (T^*)^m] \quad (3)$$

where A, *B*, *C*, and *m* are constants; *n* is the strain hardening exponent

As plastic strain accumulates and reaches failure strain, material removal takes place. The accumulation of plastic strain is covered by the Johnson-cook plasticity model, the plastic failure strain ε_f is defined by the Johnson-cook damage initiation model:

$$\varepsilon_f = \left[D_1 + D_2 e^{D_3 \sigma^*}\right][1 + D_4 \dot{\varepsilon}^*][1 + D_5 T^*] \quad (4)$$

where D_1, D_2, D_3, D_4 and D_5 are fracture model constant. σ^* is the stress triaxially factor and $\dot{\varepsilon}^*$ is strain rate.

Table 6 General properties of CRFP and Johnson-cook fracture model for the brittle material [21]

General Properties	Density (kg/m^3)		Young Modulus (Gpa)		Poisson's ratio	
	1810		294		0.24	
Johnson Cook Properties	**A(Mpa)**	**B(Mpa)**	**N**	**d1**	**d2**	**d3**
	125	1010	0.47	0.001	0.001	9.85

The frictional contact between a cross-nick tool and CFRP workpiece was modelled with a general software contact algorithm by the penalty contact method. The constant coefficient of friction of 0.3 has been used [22]. Boundary conditions for the numerical simulation was applied like the experimental works including the value of velocity as cutting motion and angular velocity of rotation of the tool. During the edge-trimming process, the workpieces were able to deflect to any degree of freedom and the motion of the X-axis was instructed by using boundary condition type *Displacement/ Rotation* (UY=UZ=RY=RZ=0). To ensure the workpiece moves linearly along the X-axis, the *Predefined Field* features were applied with displacement per unit time that served as velocity motion. Then, the rotation of the tool was designed by using boundary condition type *Velocity/Angular Velocity (VR3)* with radians per unit time, which it was rotated at Z-axis. Figure 2 summarizes the boundary conditions that applied in the numerical modelling in this research works.

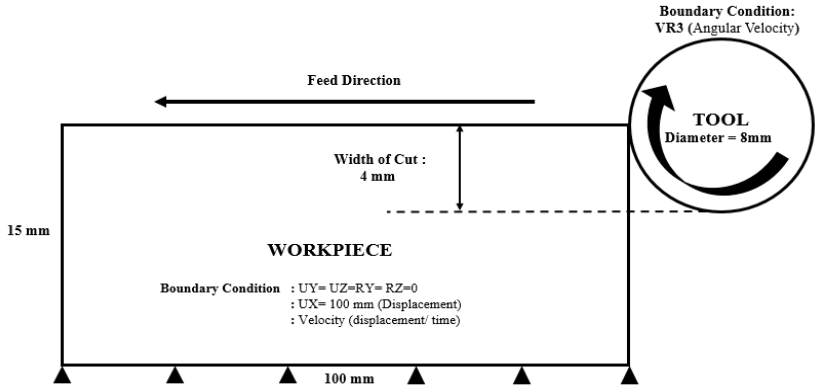

Figure 2. Schematic illustration of boundary conditions for tool and workpiece.

3. RESULTS AND DISCUSSION

3.1 Effects of Helical Features on Surface Roughness

The effects of helical features on surface roughness can be compared with the help of a surface plot as illustrated in Figure 3. All the variables and its interaction were found to be statistically significant (p-value<0.05) according to ANOVA (Table 2). According to the results, the interactions of the double helix angle highly influences, and is more dominant compared to the single helix angle either left or right referred to by the p-value. Consistent with the literature, as reported by (Haddad et al. 2014) which indicates that the groove of the second helix angle either left or right that produced a segmented helical edge directly influences the surface

roughness. Other than that, by employing this statistical method, it further supports the results of [5] which states that both cutting edges (left and right helix) take part in the cutting process. For the single helix angle, the left helix is more dominant compared to the helix right according to the p-value. The low surface roughness can be achieved when a 35° right helix angle interacts with a 12° left helix angle. The surface roughness slightly changed when using the 8° helix angle left either varying at any angle of the right helix (35° to 45°), but not for the case of the12° left helix. The surface roughness gradually increased to a maximum value by increasing the right helix angle as found for the12° left helix. The reason for this circumstance is probably due to the high shearing angle through one of the cutter peripheries that increases the contact friction between the cutting tool and the machined surface, thus increasing the chip temperature. The chip is usually formed by plastic deformation of the respective material as its going through the shearing zone. When cutting polymers and their composites, elastic deformation play a significant role in determining the cutting forces. Due to the elastic recovery, rubbing in this zone might be substantial and the resulting temperature rise may heat the polymer matrix above the glass transition temperature, T_g which results in a significant plastic flow in this region.

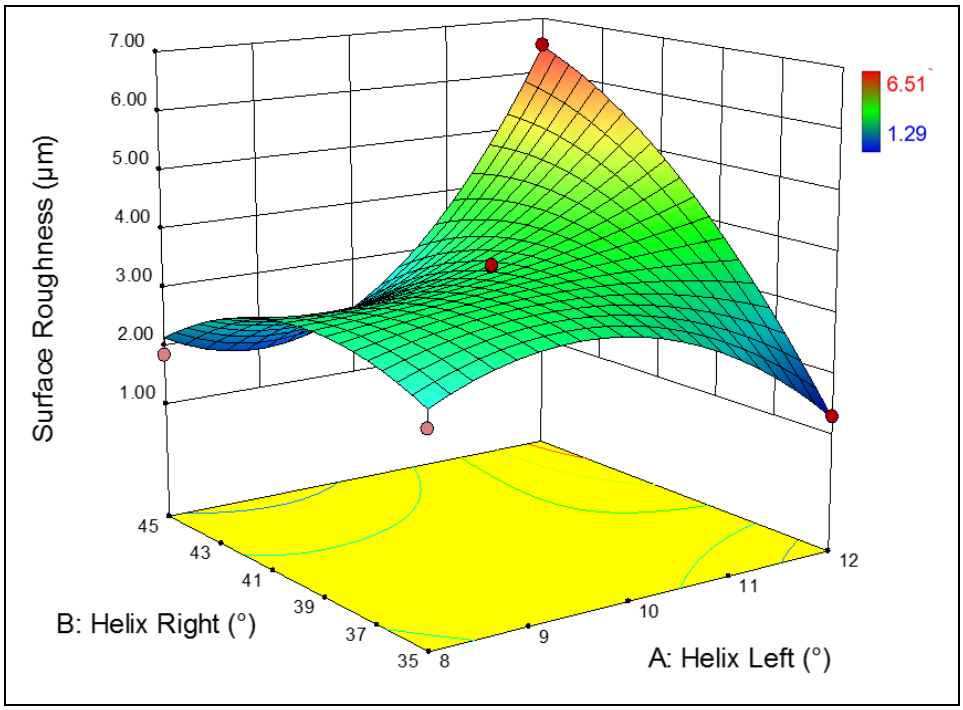

Figure 3. Surface plot of surface roughness results.

3.2 Numerical Simulation Results

The numerical simulation in this study is explored on the discovery of a double helix tool toward the plies behaviour. The results only cover visually on software and are described according to step by step damage initiated until its failure and the role of each helix angle was explained according to the simulation results. The tool model in these results has been hidden to improve the visibility of the plies behaviour during numerical simulation. Additionally, this study also found that there were chips produced during simulation of the edge-trimming process and each of the helix angles produced different quantity of chips. This quantity of chips formation has been recorded. Figure 4 shows the simulation results of the edge-trimming of CFRP by the cross-nick tool. The results covered in this numerical simulation is according to the cross-nick tool with left helix angle 7° and right helix angle 40°.

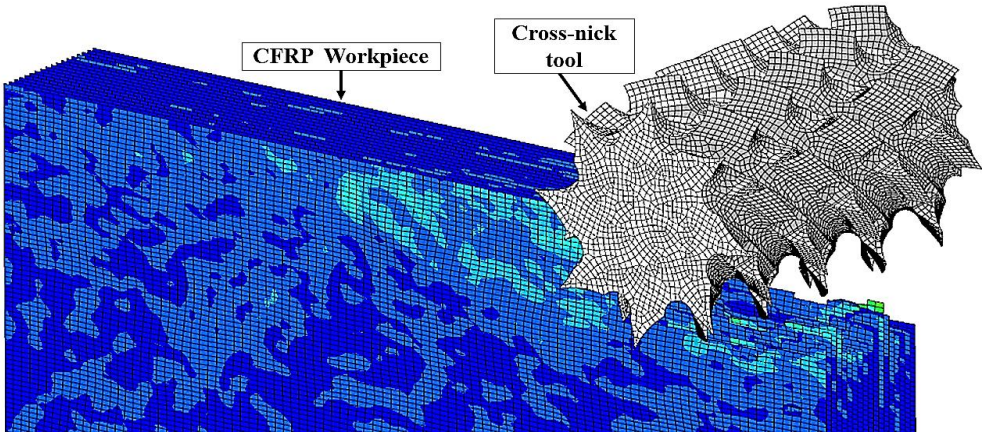

Figure 4. Numerical simulation results of edge-trimming of CFRP by cross-nick tool.

In order to understand the behaviour of the double helical features in this study, Figure 5 was used as a guidance for the explanation in Figure 6. Figure 5 illustrates the three types of view (top, side and front) about the workpiece conditions during engagement of the cross-nick tool equally in time. The side view is used to explain the phenomena of tool entry and the motion of the plies changes in the upward direction as a result from the up-milling force. Top and front view are used to explain the interference of the helix left and the right tool geometry towards the plies.

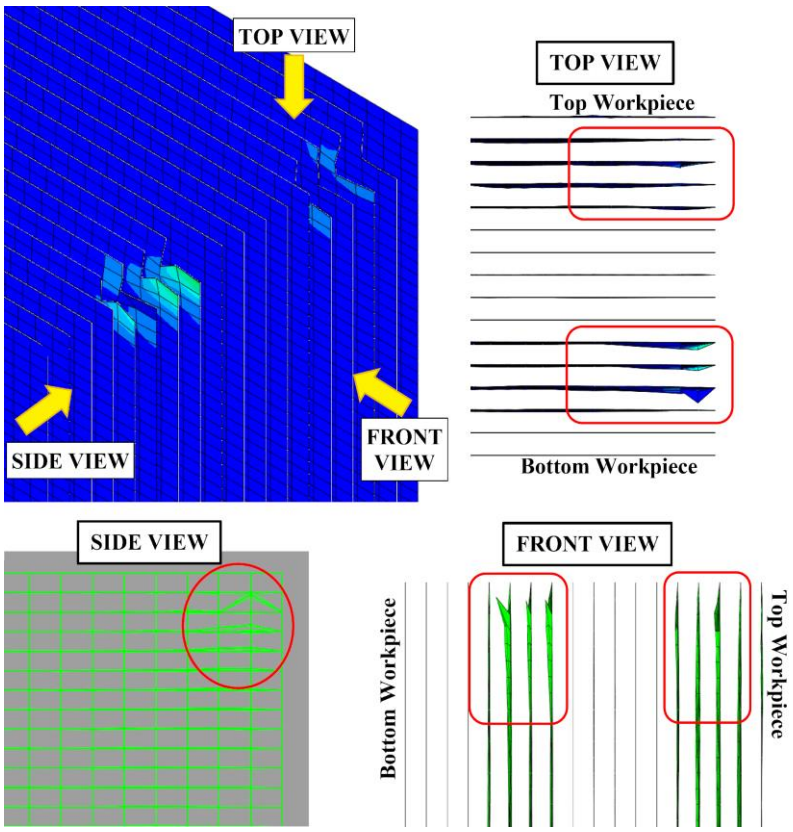

Figure 5. The top, side and front view of the machined surface.

Figure 6 illustrates the conditions of the plies whilst experiencing the edge-trimming process from the beginning several times. From the figure, the understanding about effects of the helical features is seen more clearly. In Figure 6(a), with the tools initially engaged with the plies, it was

found that the formation of the plies moved downwards (to the bottom of the workpiece) because of the effects of the right helix angle (40°). The fibres of the plies also initially encountered the stress by the tool tip at the centre of the workpieces due to the shape of the cross-nick tool. But, the fibres still did not suffer any significant damage in this stage as the pressure from the tool tip did not reach the minimum value.

Figure 6(b), shows that the formation of the plies is still in the same direction, and the left helix angle (7°) began to interfere. The left helix angle causes the plies to experience two directions of forces, which are upward and downward that can be seen in Figure 6(c). In accordance with this phenomenon, one of the possible reasons for this is the double helical tool which provides ~~a~~ clean cutting by balancing the cutting forces' magnitudes upwards and downwards on the material [23]. Lastly, Figure 6(d) shows the tool completely penetrated into the workpiece. When the nodes element exceeds a critical value of stress, the element is removed from the other nodes by using an element deletion method that is provided by the software. By comparing the left and right helix angle of the cross-nick tool, the right helix has initiated the workpieces at first followed by left helix.

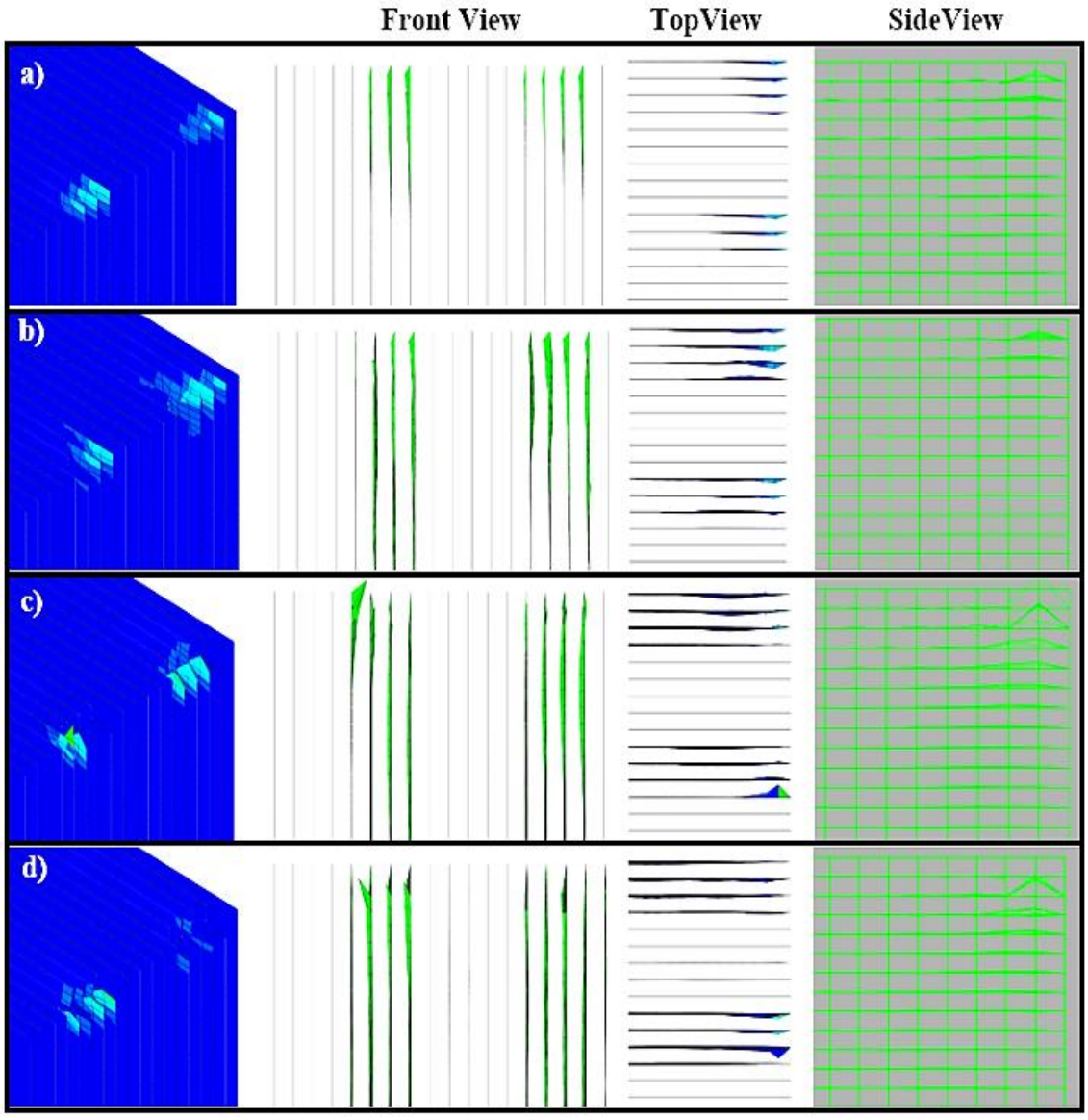

Figure 6. Plies formation due to interference of the left and right tool helical features.

In the numerical element deletion criteria, chips were produced caused by material separation through element deletion at the cutting tool tip. The formation of chips is not supposed to occur because module failure criterion is used for all node elements in the workpiece. However, this has happened due to the element deletion occurring too early on certain nodes element due to the shape of the tool geometries. Table 7 and Figure 7 shows the chips produced based on the time index of simulation.

Table 7 Chips occurrence by different tool helical features

	Right Helix	**Left Helix**
Occurrence of first chip (observed time index)	0.440	0.547
Total number of chips produced (units)	13	8

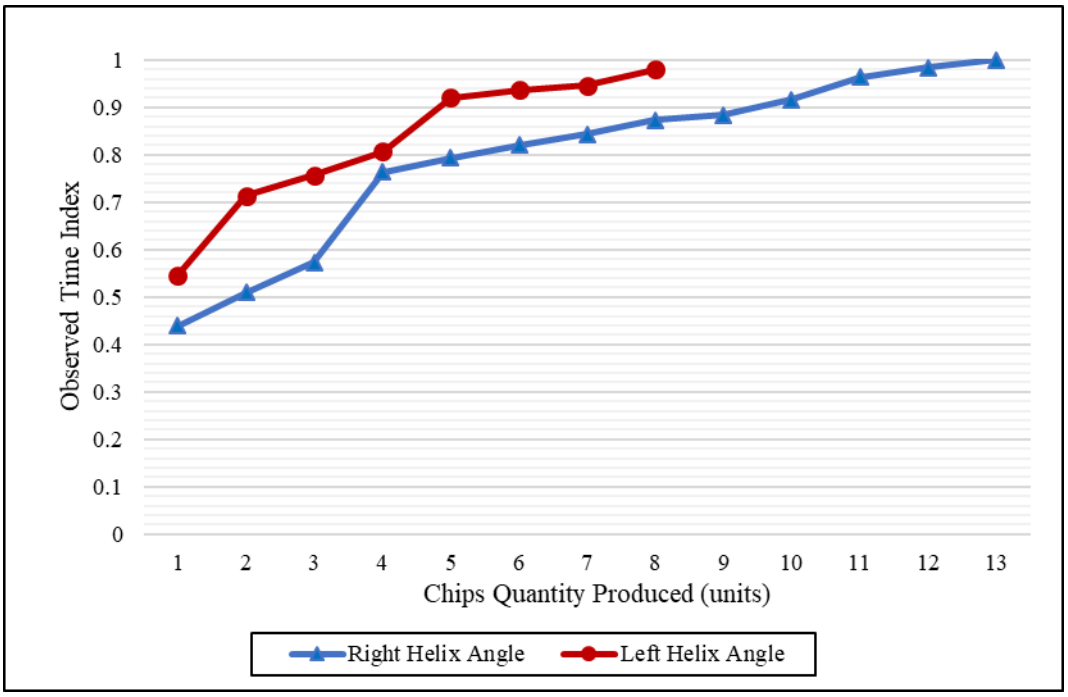

Figure 7. The number chips generated due to the right and left helix angle by means of time.

According to Figure 7 and the observations results during the simulation works, there were four stages before the chips were produced whereby the first stage focuses on the fibres deforming through the elastic region at 0.01 to 0.17 of the time index (no nodes element deleted). In the second stage, the fibres were deformed through the plastic region at 0.18 to 0.31 (no nodes element was deleted). The third stage concerning the element deletion due to the shearing by the right helical features at first than the left helical features, the element failed. The last stage revealed that the formation of chips produced by material separation resulted from element deletion due to the right and left helix angle. In addition, the results also indicated that the right helix angle as being more dominant in deforming the woven fibres plies compared to that of the left helix angle because of the occurrence of chip formation produced by the right helix earlier than the left helix angle (Figure 7 and Table 7). Besides, the quantity of chips produced by the right helix angle were found to be more than left helix angle.

These results seem to be consistent with other researchers, where it was found that the flank wear on the cutting edge of the right helix angle is worse compared to the left helix angle [5]. This circumstance reflect that the left helix serves as a secondary material removing features compared to the right helix which serves as a primary material removing feature. The right helix angle removes the material in advance rather than the left helix, which removes the excess

materials that were spared by the right helix angle as indicated by the results of the time index of both helical features. Since the left helix angle becomes the secondary material remover whereby it removes excess materials from the right helix angle, it seems to be able to clarify that the left helix angle is more dominant than the surface roughness results compared to that of the right helix angle as referred to in the ANOVA results (Table 2). As a result, the left helix angle also serves as a finishing feature on the cross-nick tool.

4. CONCLUSION

This study offers a good understanding on the influence of double helixes angle on the cross-nick tool in the edge-trimming of CFRP workpiece. The experimental works explored on the effects of the double helix angle to the surface roughness and the numerical simulation examined the sequential progression of the cross-nick tool penetrated to the workpiece. The following conclusions can be drawn:

i. Surface roughness of CFRP machined surface was statistically significant that it was dependent on both helices angle in the cross-nick tool. The combination of the left and the right helical groove produced the segmented helical edge which simultaneously trimmed the workpieces continuously.

ii. Observation on the sequence of the tools penetrated to the workpiece during simulation, exposed that the plies experienced two directions of forces which were downward and upward. The plies were pushed to the bottom of the workpiece by the right helix angle and lifted upwards to the top of the workpiece by the left helix angle.

iii. Statistical analysis approach discovered that the left helix angle highly influences the surface roughness compared to that of the right helix angle. In respect to that, the numerical simulation revealed that the left helix angle indirectly plays the role of a finishing feature in the double helix tool because it is the last helical feature that is ploughed and removed off the excess material left by the right helix angle.

ACKNOWLEDGEMENTS

The authors are grateful to Malaysian Ministry of Higher Education and Universiti Teknikal Malaysia Melaka for their technical and financial support under Prototype Research Grant Scheme No: PRGS/1/2019/TK03/UTEM/02/1.

REFERENCES

[1] Ghafoori, E., Motavalli, M., Nussbaumer, A., Herwig, A., Prinz, G. S., & Fontana, M. "Determination of minimum CFRP pre-stress levels for fatigue crack prevention in retrofitted metallic beams," Engineering Structures **84** (2014) 29-41.

[2] El-Hofy, M. H., S. L. Soo, D.K. Aspinwall, W. M. Sim, D. Pearson & P. Harden, "Factors Affecting Workpiece Surface Integrity in Slotting of CFRP." Procedia Engineering **19** (2011) 94–99.

[3] A. Karataş, Meltem, & H. Gökkaya, "A Review on Machinability of Carbon Fiber Reinforced Polymer (CFRP) and Glass Fiber Reinforced Polymer (GFRP) Composite Materials." Defence Technology **14** (2018) 318–326.

[4] Hosokawa, Akira, Naoya Hirose, Takashi Ueda, Tatsuaki Furumoto. "High-Quality Machining of CFRP with High Helix End Mill," CIRP Annals - Manufacturing Technology **63** issue 1 (2014) 89–92.

[5] Yang, Xiao Fan "The Analysis of Tool Wear in Milling CFRP with Different Diamond Coated Tool," Key Engineering Materials **667** (2015) 231–236.
[6] Bílek, Ondřej, Milan Žaludek, & Jiří Čop. "Cutting Tool Performance in End Milling of Glass Fiber-Reinforced Polymer Composites," Manufacturing Technology **16**, 1 (2016) 12–16.
[7] Rimpault, Xavier, Jean François Chatelain, Jolanta E. Klemberg-Sapieha, & Marek Balazinski. "Surface Profile Topography of Trimmed and Drilled Carbon/Epoxy Composite," Procedia CIRP **45** (2016) 27–30.
[8] Tebassi, Hamid, *et al.* "Quality-Productivity Decision Making When Turning of Inconel 718 Aerospace Alloy: A Response Surface Methodology Approach," International Journal of Industrial Engineering Computations **8**, 3 (2017) 347–62.
[9] M. A. Amran, S. Salmah, N. I. S. Hussein, R. Izamshah, M. Hadzley, Sivaraos, M. S. Kasim, M. A. Sulaiman, "Effects of machine parameters on surface roughness using response surface method in drilling process", The Malaysian International Tribology Conference 2013, MITC2013, Procedia Engineering **68** (2013) 24 – 29.
[10] Amran M., Izamshah R., Hadzley M., Shahir M., Amri M., Sanusi M., Hilmi H., "The Effect of Binder on Mechanical Properties of Kenaf Fibre/Polypropylene Composites Using Full Factorial Method", Applied Mechanics and Materials **695** (2015) 709–712.
[11] Kumar, Krishan, & M. L. Aggarwal. "Computer Aided FEA Simulation of EN45A Parabolic Leaf Spring." International Journal of Industrial Engineering Computations **4**, 2 (2013) 297–304.
[12] R. Izamshah, M Zulhairy, MS Kasim, M Hadzley, M Amran & M Amri. "Cutter path strategies for shoulder milling of thin deflecting walls," Adv. Mat. Res. **903** (2014) 175-180.
[13] Teimouri, V., & M. Safarabadi. "Finite Element Prediction of Curing Micro-Residual Stress Distribution in Polymeric Composites Considering Hybrid Interphase Region," Engineering Solid Mechanics **6**, 1 (2018) 11–20.
[14] Shetty, Nagaraja, S. M. Shahabaz, S. S. Sharma, & S. Divakara Shetty, "A Review on Finite Element Method for Machining of Composite Materials," Composite Structures **176** (2017) 790–802.
[15] Mark J. Anderson, Patrick J. Whitcomb. RSM Simplified: Optimizing Processes Using Response Surface Methods for Design of Experiments. 2nd Edition. Productivity Press, (2016)
[16] Jinyang Xu, Min Ji, Ming Chen & Fei Ren, "Investigation of minimum quantity lubrication effects in drilling CFRP/Ti6Al4V stacks," Materials and Manufacturing Processes **34**, 12 (2019) 1401-1410.
[17] Bernardin, Petr, Josef Vacík, Tomáš Kroupa, & Radek Kottner. "Determination of the Mechanical Parameters of a Bonded Joint between a Metal and a Composite by Comparing Experiments with a Finite-Element Model," Materiali in Tehnologije **47**, 4 (2013) 417–421.
[18] Hashin, Z., & A. Rotem. "A Fatigue Failure Criterion for Fiber Reinforced Materials." Journal of Composite Materials **7**, 4 (1973) 448–464.
[19] Hashin, Z. "Failure Criteria for Unidirectional Fibre Composites." Journal of Applied Mechanics **47** (1980) 329–334.
[20] Soldani, X., C. Santiuste, A. Muñoz-Sánchez, & M. H. Miguélez, "Influence of Tool Geometry and Numerical Parameters When Modeling Orthogonal Cutting of LFRP Composites," Composites Part A: Applied Science and Manufacturing **42**, 9 (2011) 1205–1216.
[21] Sause, M. G. R., & S. Horn. "Simulation of Acoustic Emission in Planar Carbon Fiber Reinforced Plastic Specimens." Journal of Nondestructive Evaluation **29**, 2 (2010) 123–142.
[22] Phadnis, Vaibhav A., Farrukh Makhdum, Anish Roy, & Vadim V. Silberschmidt. "Drilling in Carbon/Epoxy Composites: Experimental Investigations and Finite Element Implementation." Composites Part A: Applied Science and Manufacturing **47** (2013) 41–51.
[23] Lorincz, Jim. "No Two CFRP Materials Machine Exactly Alike." Manufacturing Engineering **157**, 3 (2016) 81–88.